Diacritic Binding of an Indenoindole Inhibitor by CK2α Paralogs Explored by a Reliable Path to Atomic Resolution CK2α' Structures

Dirk Lindenblatt, Anna Nickelsen, Violetta M Applegate, Jennifer Hochscherf, Benedict Witulski, Zouhair Bouaziz, Christelle Marminon, Maria Bretner, Marc Le Borgne, Joachim Jose, et al.

▶ **To cite this version:**

Dirk Lindenblatt, Anna Nickelsen, Violetta M Applegate, Jennifer Hochscherf, Benedict Witulski, et al.. Diacritic Binding of an Indenoindole Inhibitor by CK2α Paralogs Explored by a Reliable Path to Atomic Resolution CK2α' Structures. ACS Omega, 2019, 4 (3), pp.5471-5478. 10.1021/acsomega.8b03415 . hal-02077897

HAL Id: hal-02077897
https://hal.science/hal-02077897

Submitted on 24 Mar 2019

HAL is a multi-disciplinary open access archive for the deposit and dissemination of scientific research documents, whether they are published or not. The documents may come from teaching and research institutions in France or abroad, or from public or private research centers.

L'archive ouverte pluridisciplinaire **HAL**, est destinée au dépôt et à la diffusion de documents scientifiques de niveau recherche, publiés ou non, émanant des établissements d'enseignement et de recherche français ou étrangers, des laboratoires publics ou privés.

This is an open access article published under an ACS AuthorChoice License, which permits copying and redistribution of the article or any adaptations for non-commercial purposes.

ACS OMEGA

Article

Cite This: ACS Omega 2019, 4, 5471−5478

http://pubs.acs.org/journal/acsodf

Diacritic Binding of an Indenoindole Inhibitor by CK2α Paralogs Explored by a Reliable Path to Atomic Resolution CK2α′ Structures

Dirk Lindenblatt,[†] Anna Nickelsen,[‡] Violetta M. Applegate,[†] Jennifer Hochscherf,[†] Benedict Witulski,[†] Zouhair Bouaziz,[§] Christelle Marminon,[§] Maria Bretner,[∥] Marc Le Borgne,[§] Joachim Jose,[‡] and Karsten Niefind*[,†]

[†]Department für Chemie, Institut für Biochemie, Universität zu Köln, Zülpicher Straße 47, D-50674 Köln, Germany

[‡]Institut für Pharmazeutische und Medizinische Chemie, Westfälische Wilhelms-Universität Münster, PharmaCampus, Corrensstr. 48, D-48149 Münster, Germany

[§]EA 4446 Bioactive Molecules and Medicinal Chemistry, SFR Santé Lyon-Est CNRS UMS 3453 - INSERM US7, Faculté de Pharmacie-ISPB, Université Claude Bernard Lyon 1, 8 Avenue Rockefeller, F-69373 Lyon Cedex 8, France

[∥]Faculty of Chemistry, Warsaw University of Technology, Noakowskiego 3, 00-664 Warsaw, Poland

Supporting Information

ABSTRACT: CK2α and CK2α′ are the two isoforms of the catalytic subunit of human protein kinase CK2, an important target for cancer therapy. They have similar, albeit not identical functional and structural properties, and were occasionally reported to be inhibited with distinct efficacies by certain ATP-competitive ligands. Here, we present THN27, an indeno[1,2-*b*]indole derivative, as a further inhibitor with basal isoform selectivity. The selectivity disappears when measured using CK2α/CK2α′ complexes with CK2β, the regulatory CK2 subunit. Co-crystal structures of THN27 with CK2α and CK2α′ reveal that subtle differences in the conformational variability of the inter-domain hinge region are correlated with the observed effect. In the case of CK2α′, a crystallographically problematic protein so far, this comparative structural analysis required the development of an experimental strategy that finally enables atomic resolution structure determinations with ab initio phasing of potentially any ATP-competitive CK2 inhibitor and possibly many non-ATP-competitive ligands as well bound to CK2α′.

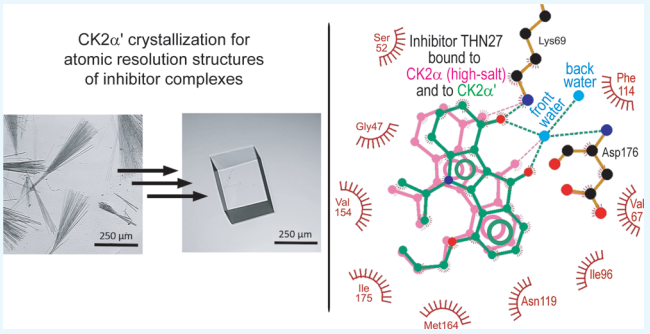

INTRODUCTION

Vertebrate genomes encode two paralogs of the catalytic subunit of protein kinase CK2 referred to as CK2α and CK2α′. They are the products of the CSNKA1 and CSNK2A2 genes, which are two of 517 eukaryotic protein kinase (EPK) genes in *Homo sapiens*.[1] The knockout of CK2α in mice prevents the development of viable animals;[2] in contrast, knocking out CK2α′ merely leads to infertile males because of severe globozoospermia.[3] The main physiological interaction partner of CK2α and CK2α′ is CK2β, a homodimer that recruits two catalytic chains to form a $CK2\alpha_2/\alpha'_2\beta_2$ holoenzyme.[4]

CK2 is biomedically relevant in particular for cancer therapy.[5] Therefore, it is subject of considerable efforts to design effective and selective inhibitors,[6−9] most of them being ATP competitive. Currently, with silmitasertib (CX-4945; Chart 1f),[9] one such CK2 inhibitor is part of a clinical phase-2 study (clinicaltrials.gov/ct2/show/NCT02128282). CK2 inhibition experiments are typically performed exclusively with either CK2α or with the CK2α-based holoenzyme, and the structure determination of enzyme/inhibitor complexes normally relies on co-crystallization with CK2α rather than CK2α′. As a consequence, it has been only rarely reported that a compound showed a significant efficacy difference between the isoforms.[10−12] The most comprehensive investigation of this type, which revealed a general tendency of natural flavonoids to inhibit CK2α′ more strongly than CK2α, was published only recently.[12]

RESULTS AND DISCUSSION

The study we present here originates from a similar feature observed for a derivative of the indeno[1,2-*b*]indole scaffold (Chart 1a,c). Several indeno[1,2-*b*]indole-type molecules were described to be effective CK2 inhibitors[13−15] without isoform selectivity. However, in the case of 5-isopropyl-4-[(prop-2-en-1-yl)oxy]-5,6,7,8-tetrahydroindeno[1,2-b]indole-9,10-dione (THN27; Chart 1c), we found an approximately 2-fold stronger inhibition effect for CK2α′ (IC_{50} = 273 nM) than for CK2α (IC_{50} = 607 nM) (Figure 1a). The binding of CK2β,

Received: December 5, 2018
Accepted: February 14, 2019
Published: March 19, 2019

Downloaded via UNIV CLAUDE BERNARD LYON 1 on March 24, 2019 at 13:23:57 (UTC).
See https://pubs.acs.org/sharingguidelines for options on how to legitimately share published articles.

© 2019 American Chemical Society

DOI: 10.1021/acsomega.8b03415
ACS Omega 2019, 4, 5471−5478

Chart 1. (a) Principle Indeno[1,2-*b*]indole Scaffold with Atom Numbering and Ring Labeling and (b–f) the CK2 Inhibitors[9,13,16] Used in This Study

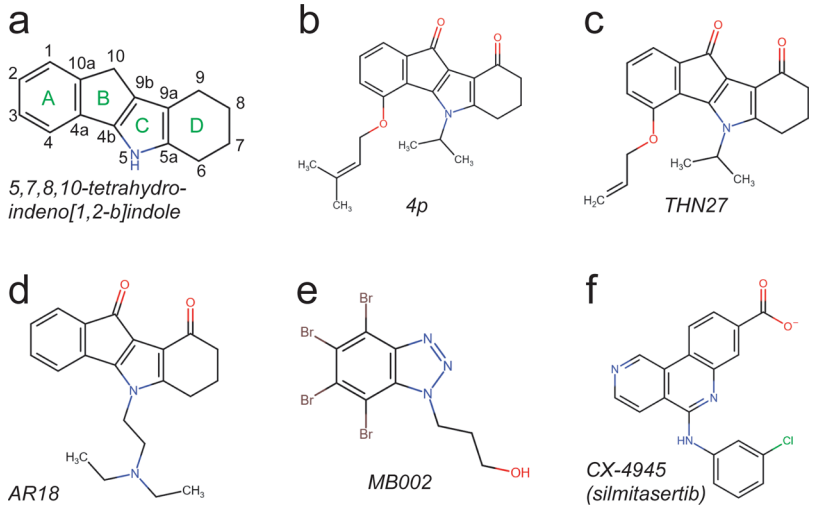

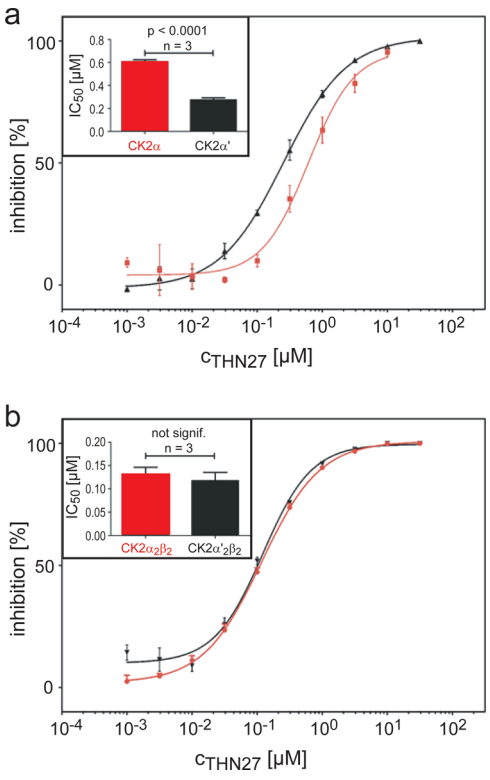

Figure 1. Differential inhibitory effect of THN27 on CK2α and CK2α'. (a) Dose-response curves of CK2α (red) and CK2α' (black) for the inhibition with THN27. (b) Dose-response curves of the holoenzymes CK2$\alpha_2\beta_2$ (red) and CK2$\alpha'_2\beta_2$ (black) for the inhibition with THN27. For each dose-response curve in (a) and (b), one example out of three replicates is shown. The histograms in the insets provide averages of all replicates together with the results of a statistical evaluation of their differences via an unpaired *t*-test.

meaning catalyzing the kinase reaction with either a CK2α- or CK2α'-based holoenzyme rather than the unbound catalytic subunit, balances the difference (Figure 1b), a feature that was reported for CK2-inhibitory flavonoids as well.[12]

This equalizing effect of CK2β made a project to optimize the basal isoform selectivity of THN27 not very promising. Therefore, rather than working out comprehensive structure–activity relationships, we decided to investigate whether the diacritic binding of THN27 by the two CK2α paralogs is correlated with structural differences.

On a level of primary structures, the two isoforms are 86% identical in the canonical EPK catalytic core (Figure 2). In particular at the ATP site, some CK2α typical bulky side chains such as Val67 or Ile175, which are known to determine the inhibitory selectivity with respect to other members of the EPK superfamily[17] (gray shadows in Figure 2), are fully conserved in CK2α'; the only sequence variation in the ATP-binding region refers to two residues of the hinge (His114 and Val115 in CK2α vs. Tyr115 and Ile116 in CK2α'; Figure 2) connecting the two main structural domains (lobes) of the kinase. This hinge region often contributes to the binding of cosubstrate or cosubstrate-competitive molecules via hydrogen and halogen bonds;[18,19] however, the polar interactions between ligand and hinge are only made with main chain atoms. In consequence, an impact of a sequence variation in the hinge region appears to be not evident, especially because the first crystallographic analysis of an indeno[1,2-*b*]indole-type inhibitor, the THN27 similar compound 4p (Chart 1b), with CK2α and CK2α' has revealed that no hydrogen bonds between the hinge backbone and the inhibitor are formed.[13]

To gain deeper insight into the structural differences between CK2α and CK2α' upon binding of THN27 (Chart 1c), we solved corresponding co-crystal structures (Table S1, structures 1, 2, and 4). For CK2α, more precisely for the C-terminal truncation construct CK2α^{1-335},[20] it was comparatively straightforward to determine two complex structures of acceptable quality. They resulted either from a "high-salt" (precipitant: 4.1 M NaCl) or from a "low-salt" crystallization condition (precipitant: 30% poly(ethylene glycol) 8000) (Table S1, structures 1 and 2). Human CK2α, in contrast to CK2α' or other CK2α homologs, is well known for its crystalline polymorphism. It depends among others on the salt concentration of the crystallization medium and is accompanied with local conformational changes in the ATP site region;[13,19,21] therefore, the use of two different crystallization media was intended to get a comprehensive structural picture of THN27 binding similar to the approach recently described for 4p.[13]

DOI: 10.1021/acsomega.8b03415
ACS Omega 2019, 4, 5471–5478

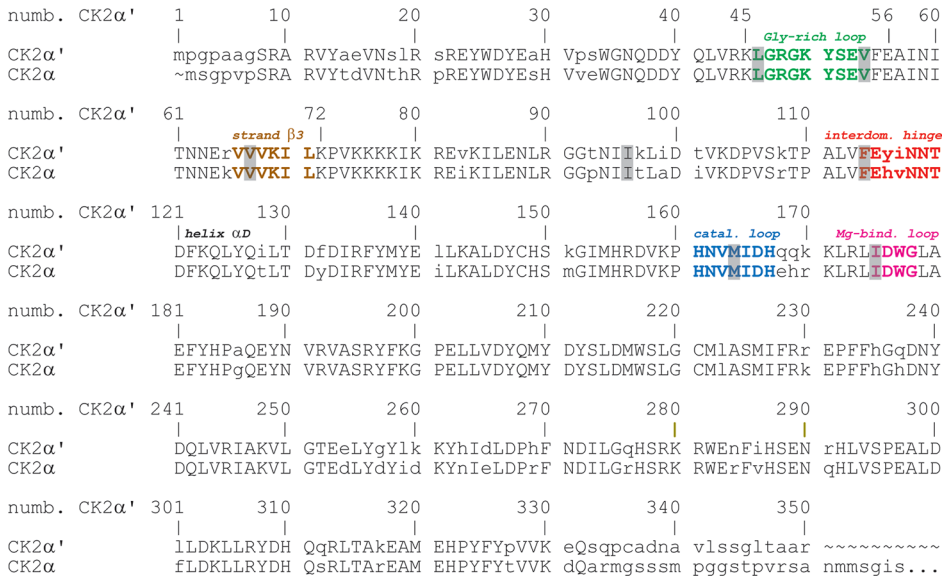

Figure 2. Sequence alignment of human CK2α and CK2α'. Identical positions are printed with capitals. Regions contributing to the ATP-binding site are indicated by different colors: the glycine-rich loop in green, the strand β3 in brown, the interdomain hinge in red, the catalytic loop in blue, and the magnesium-binding loop in magenta. Large side chains restricting the space at the ATP site[17] are highlighted with gray shadows.

For crystallization of CK2α', we used the point mutant CK2α'^{C336S}.[16,19] Here, we were faced with a problem described earlier[16] that has restricted the CK2α' structures published so far to a relatively small number:[13,16,19,23,24] CK2α' crystallizes easily under a variety of conditions but typically as showers or bundles of rather tiny and essentially unusable needles (top-left corner of Figure 3a). To some extent, we had overcome this problem previously by screening various CK2 inhibitors as CK2α'^{C336S} crystallization additives, which had identified 3-(4,5,6,7-tetrabromo-1*H*-benzotriazol-1-yl)propan-1-ol (MB002; Chart 1e) as the most effective hit.[16] For this study, we refined that approach by several steps of standard micro- and macroseeding and most importantly, by increasing the lithium chloride content of the crystallization drop. The optimal LiCl concentration after equilibration was in the range of 0.7 to 0.9 M. The optimized procedure allowed us to grow large well-shaped CK2α'/MB002 crystals (top-right corner of Figure 3a) in a reproducible way.

These CK2α'/MB002 crystals are most valuable tools to determine high-quality CK2α' complex structures because of a number of properties: (i) their diffraction power is excellent with standard synchrotron beamlines leading reliably to diffraction data sets of 1.0 ± 0.1 Å resolution as shown in this study (Table S1), (ii) this high resolution enables ab initio structure determination, thus avoiding any model bias from known CK2α or CK2α' structures, for example, all four CK2α' structures of this study (Table S1, structures 3−6) were solved via ab initio phasing, (iii) the crystals are reasonably robust and tolerate transfer and soaking steps fairly well, (iv) the ATP site is fully accessible in the crystal packing, which permits to replace the original MB002 inhibitor by exhaustive ligand exchange; because of the size of the crystals, the penetration of colored inhibitors such as THN27 to the center of the crystal body is easily observable under a microscope, which provides a preliminary indication of binding; whether this binding is specific that must be validated by a difference fourier map or, as done in this study, by an electron density calculated after ab initio phasing, and (v) with about 250 μm in each dimension (top-right corner of Figure 3a), the crystals are not at their limit. Rather, larger CK2α'/inhibitor crystals can be grown in the indicated way up to a size suitable for neutron diffraction studies. Neutron diffraction enables the experimental determination of precise hydrogen atom positions, which are potentially beneficial for the in silico design and optimization of CK2 inhibitors.

To test the power of the procedure, we determined CK2α' co-crystal structures not only with the MB002 ligand and with our selective target molecule THN27 but also with two inhibitors of either higher or lower affinity. The latter was the indeno[1,2-*b*]indole-type compound AR18 with a large substituent at ring C instead of ring A (Chart 1d). This kind of variation of the indeno[1,2-*b*]indole framework is an efficient way to weaken the affinity to CK2 while simultaneously improving the binding to a former off target, the breast cancer resistance protein ABCG2, which is an ABC half transporter overexpressed in breast cancer cells.[28] AR18 is an intermediate of these polypharmacology efforts. As a high-affinity ligand, we chose the benchmark CK2-inhibitor CX-4945[9] (Chart 1f) for which no CK2α' structure is available so far. Whereas CX-4945 replaces MB002 completely within 2 days of crystal soaking (Figure 3), an increasing degree of occupation with soaking time could be observed for AR18 and THN27. After 7 days, it was more than 90% for either AR18 or THN27, leaving only small amounts of residual electron density that did not disturb the structure refinement later. In each of the three cases, a reference structure determined by co-crystallization rather than soaking and ligand exchange was superimposed: for CX-4945, a complex structure with CK2α (3NGA),[22] and for AR18 and for THN27, the CK2α' structure 5OOI[13] containing the indeno[1,2-b]indole-type inhibitor 4p, which differs from THN27 by two additional methyl groups at the ring A substituent (Chart 1b). These overlays show close coincidences of the bound inhibitors (Figure 3d) or at least their central scaffolds (Figure 3b,c). Thus, the replacement procedure outlined in Figure 3 leads to reliable results, and it is a promising and generally applicable strategy to determine atomic resolution structures of CK2α'

DOI: 10.1021/acsomega.8b03415
ACS Omega 2019, 4, 5471−5478

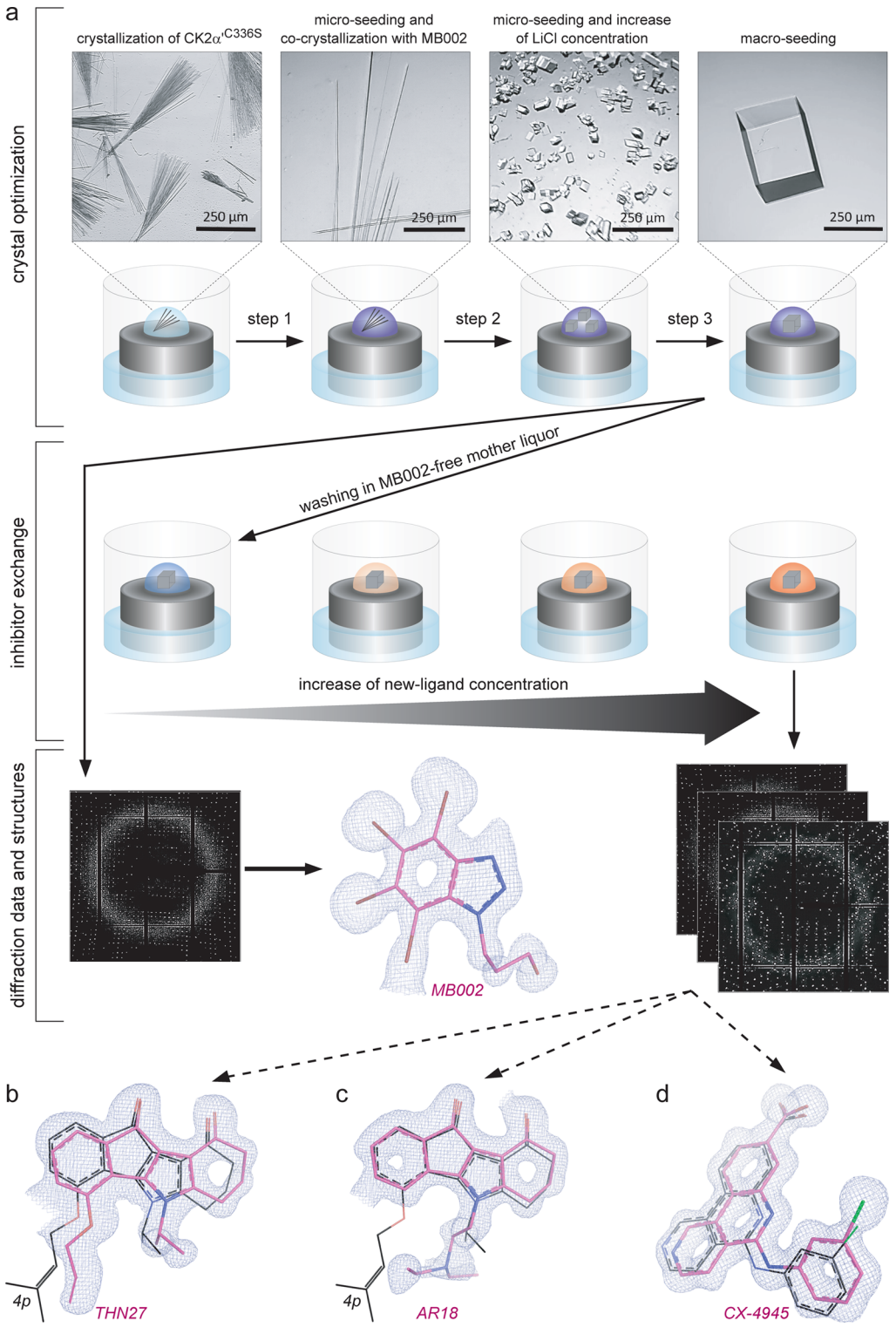

Figure 3. General strategy to determine atomic resolution ab initio structures of CK2α' complexes with ATP-competitive inhibitors. (a) Outline of the procedure with the CK2α'/MB002 structure as primary result. The replacement inhibitors: (b) THN27, (c) AR18, and (d) CX-4945. For comparison, structures of CK2α' with the indeno[1,2-b]indole-type inhibitor 4p[13] (b, c) or of CK2α with CX-4945[22] (d) were overlaid. 4p and CX-4945 are drawn with black C-atoms. The four inhibitors are displayed in their final electron densities with cutoff levels of 1.5 σ for (a), (b), (d) or 1.0 σ for (c).

complexes with essentially any ATP-competitive CK2 inhibitor and possibly with further small molecule ligands of CK2.

The CK2α'/MB002 structure is the highest-resolved X-ray structure of a protein kinase published to date. One of its remarkable details not visible in a lower resolution structure of this complex (3OFM)[16] is a pairwise ambiguity of the side chains of Phe122 and Tyr126 in the small helix αD. Each of them can adopt an "out"- or an "in"-conformation. This leads to the combinations Phe122-out/Tyr126-in (blue electron density in Figure 4a), which is prevailing in the CK2α'/MB002

DOI: 10.1021/acsomega.8b03415
ACS Omega 2019, 4, 5471−5478

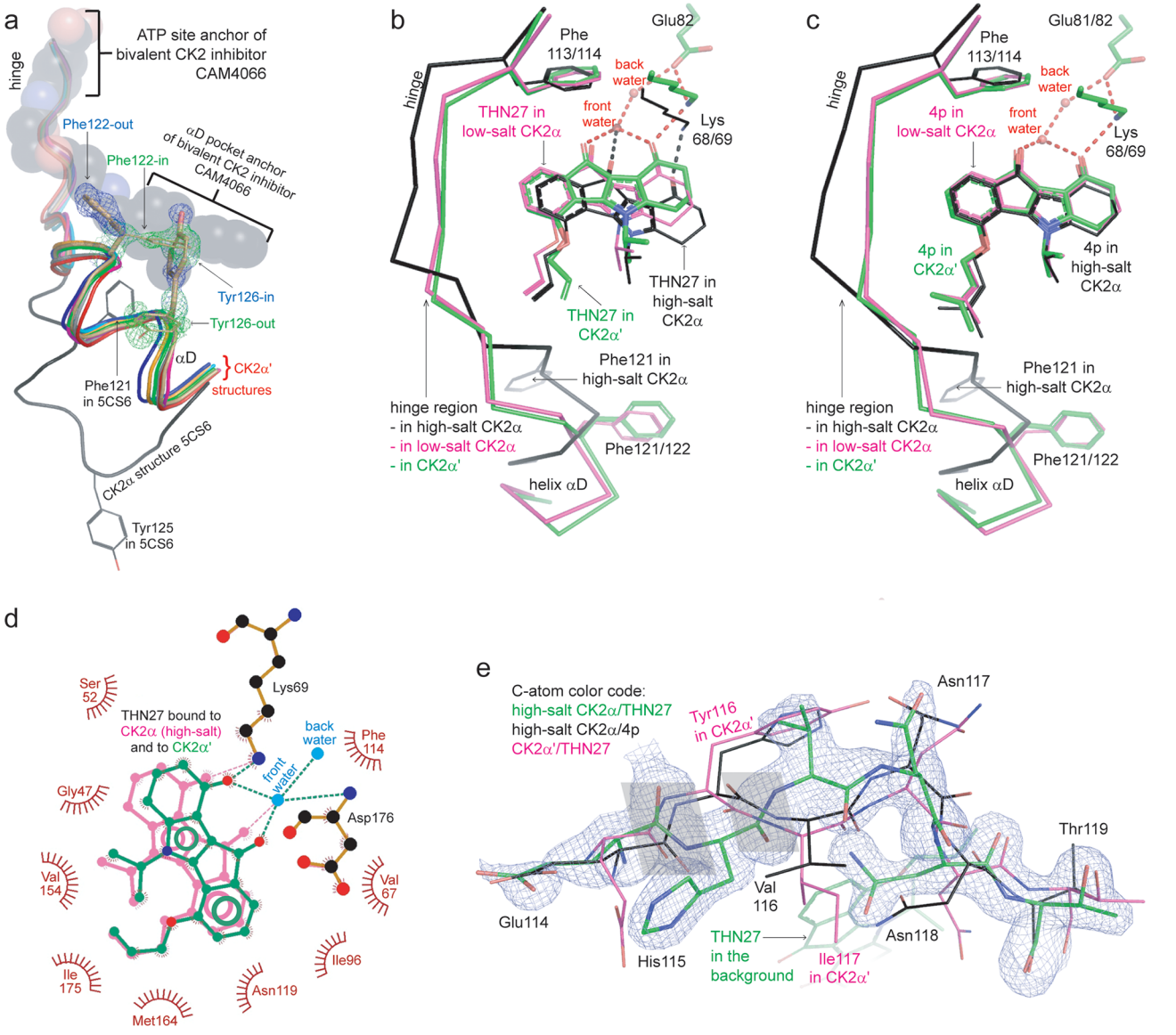

Figure 4. Structural observations in complexes of CK2α' and CK2α with MB002 and THN27. (a) Pairwise ambiguity of the helix αD residues Phe122 and Tyr126 in the CK2α'/MB002 complex, visible by alternate side chain conformations in direct vicinity of the αD pocket. The two alternate rotamers of Phe122 and Tyr 126 are embedded in either green or blue electron densities (cutoff level 1 σ). The αD pocket is indicated by the bivalent CK2 inhibitor CAM4066[25] (PDB 5CU4), which is drawn with transparent spheres. The indeno[1,2-*b*]indole-type inhibitors (b) THN27 and (c) 4p bound to CK2α' (green C-atoms), to low-salt CK2α (magenta-colored C-atoms) and to high-salt CK2α (black C-atoms), are drawn after superimposition of the enzyme matrices. The hydrogen bond networks around two conserved water molecules[26] typical for the binding of indeno[1,2-*b*]indole-type inhibitors[13] are indicated by magenta-colored dotted lines. The two black dotted lines in the high-salt CK2α/THN27 complex (b) show the remaining hydrogen bonds of THN27 after an H-bond loss after rotation of the inhibitor. (d) 2D-projection (LIGPLOT)[27] of the noncovalent interactions between THN27 and either CK2α' (THN27 with green C-atoms) or CK2α (high-salt structure; THN27 with magenta-colored C-atoms). (e) Peptide switches (highlighted by gray parallelograms) and side chain movements at His115 and Val116 of CK2α documented by final electron density (cutoff level 1 σ) lead to a novel hinge conformation in the high-salt CK2α/THN27 complex.

structure, or Phe122-in/Tyr126-out (green electron density in Figure 4a), which is less occupied. The respective in-rotamer of the side chains overlaps slightly with the so-called "αD pocket". This is an allosteric site so far exclusively known from CK2α where it can be exploited for the design of highly selective CK2 inhibitors.[25,29] Some of them are bivalent molecules such as CAM4066 (Figure 4a) with an anchor group for the ATP site and a second one for the αD pocket.

The occupation of the αD pocket by a small molecule requires that neither Phe121 nor Tyr125 (the CK2α equivalents of Phe122 and Tyr126 in CK2α') are directed inward. In CK2α, this can be achieved either by out-conformations of those side chains or by backbone rearrangements in the helix αD region or by combinations of these as exemplified by the CK2α structure 5CS6[25] (black ribbon in Figure 4a). The essential hinge/helix αD flexibility required for accessibility of the αD pocket is known for a long time for CK2α.[21,30,31] It was confirmed by in silico simulations with CK2α,[32,33] but it was never observed in the case of CK2α' where the hinge/helix αD backbones of available structures are rigid and coincide in a fairly narrow range. This was shown recently for seven CK2α' chains,[13] and it is confirmed here for the four high-resolution CK2α' structures of this study (Figure 4a). Does this mean that in CK2α', in contrast to CK2α, the

DOI: 10.1021/acsomega.8b03415
ACS Omega 2019, 4, 5471−5478

αD pocket is inaccessible for inhibitory compounds? Is therefore the αD pocket rather than the ATP site the key region for the design of isoform selective CK2 inhibitors? These questions must remain open at the moment, but it is at least remarkable in this context that the CK2α′/MB002 structure of this work provides the first indication that, irrespective of a rigid helix αD backbone, a limited side chain flexibility next to the αD pocket exists (Figure 4a). Whether this flexibility is sufficient to permit an out/out-rotamer combination of the Phe122/Tyr126 couple and thus to open the αD pocket of CK2α′ for suitable small molecules, this must be clarified by enzymological and crystallographic experiments.

To detect structural reasons for the conspicuous differential inhibitory efficacy of THN27 (Figure 1a), we compared the three THN27 complex structures of this work (Table S1, structures 1, 2, and 4) among each other (Figure 4b) and with three published CK2α/CK2α′ structures in complex with 4p (Figure 4c).[13] Overall, a remarkable "oxygen-in"/"hydrophobic-out" binding mode that was recently described for 4p[13] is confirmed by THN27 (and by AR18 as well): whereas the inhibitor does not form any hydrogen bond with the hinge region, its two ketonic oxo groups (Chart 1c) participate in a solvent inaccessible hydrogen bond network that involves two conserved water molecules[26] (front and back water in Figure 4b−d) as well as Lys69 and Glu82, two residues conserved likewise (Figure 4b,c).

4p serves as a reference here because its orientation within the ATP site and its anchoring by three H-bonds is maintained in detail (Figure 4c), irrespective of the harboring enzyme isoform, the crystallization conditions (high or low salt) and the crystal packing; even structural variations of the neighboring hinge/helix αD region, which can occur if CK2α serves as the host enzyme,[21] have no impact on 4p binding. The coordination of THN27, however, is significantly more variable (Figure 4b) in the CK2α′/THN27 and in the low-salt CK2α/THN27 complex (green- and magenta-colored C-atoms in Figure 4b); the THN27 binding is equivalent to the 4p complexes in Figure 4c, whereas in its high-salt structure with CK2α (black C-atoms in Figure 4b), THN27 is significantly rotated outward. This means that only two of its originally three H-bonds remain (black dotted lines in Figure 4b). This loss of one H-bond is schematically depicted in Figure 4d.

In parallel to this, in direct proximity to the bound THN27 inhibitor, a novel conformation of the interdomain hinge that was never observed before for CK2α was trapped in the high-salt CK2α/THN27 structure. This is a remarkable feature against the following background: the aforementioned conformational flexibility of the hinge/helix αD region of human CK2α[21,25,30,31] mainly refers to the helix αD, whereas the interdomain hinge in a strict sense (red in Figure 2) usually accompanies these adaptations by moving as a rigid group of low internal dynamics. The standard conformation of the hinge is found in the high-salt CK2α/4p complex, in the CK2α′/THN27 complex (black and magenta-colored C-atoms in Figure 4e), and in all other structures of this study with one exception. This exception is the high-salt CK2α/THN27 structure (green C-atoms in Figure 4e) where unprecedented peptide switches accompanied with large shifts and reorientations of the enclosed side chains can be observed. A comparison of the two high-salt CK2α structures suggests that these conspicuous structural changes are not enforced by the high salt concentration; rather, they seem to reflect subtle impacts of the nearby THN27 ligand. Remarkably, this conformational variability concerns His115 and Val116 (Figure 4e), that is, exactly those two residues that make up the only sequence differences between CK2α and CK2α′ in the ATP site neighborhood (Figure 2). Tyr116 and Ile117, the CK2α′ equivalents, are significantly larger, less flexible, and thus presumably stabilizing factors of the standard hinge conformation as it was observed in CK2α′ structures so far exclusively.

In summary, with CK2α′ as a docking partner, THN27 encounters a conformationally stable enzyme environment with a binding site preformed to coordinate the compound in the typical indeno[1,2-*b*]indole binding mode known from 4p.[13] The CK2α isoform, however, is conformationally dynamic in the hinge/helix αD region as an essential part of the ATP site environment and does not provide a preformed conformation for THN27 binding. Thus, either structural adaptations of CK2α are necessary for optimal THN27 binding or THN27 partially binds in a nonoptimal mode, that is, with a reduced number of enzyme-inhibitor H-bonds (Figure 4d). These structural features correlate well with the higher inhibitory impact of THN27 on CK2α′ than that on CK2α, which we observed (Figure 1a) and was reported for certain inhibitory benzimidazole derivatives[11] and for natural flavonoid inhibitors[12] as well.

However, it seems to be unlikely that this slight preference of THN27 for CK2α′ can be extended toward a CK2 inhibitor with strong isoform selectivity. The reason is that CK2β binding to CK2α′ and CK2α removes the IC_{50} difference of THN27 (Figure 1b) as reported similarly for flavonoid-type CK2 inhibitors[12] and that the CK2β-bound form of CK2α/CK2α′ is the dominating CK2 entity in cells.[34] Most probably, CK2β exerts this equalizing effect by stabilization of the hinge conformation. Comparative structural analyses of significant $CK2\alpha_2\beta_2$- and $CK2\alpha'_2\beta_2$-holoenzyme complexes are required to validate this hypothesis.

■ ASSOCIATED CONTENT

Supporting Information

The Supporting Information is available free of charge on the ACS Publications website at DOI: 10.1021/acsomega.8b03415.

> Crystallization conditions, X-ray diffraction data, and refinement statistics, suppliers of materials, and details to experimental and computational methods (chemical synthesis and analytics, protein preparation, enzyme kinetics, and protein crystallography procedures) (PDF)

Accession Codes

The PDB codes of the six structures are given in Table S1.

■ AUTHOR INFORMATION

Corresponding Author

*E-mail: Karsten.Niefind@uni-koeln.de. Tel: +49 221 470 6444. Fax: +49 221 470 3244.

ORCID

Marc Le Borgne: 0000-0003-1398-075X

Karsten Niefind: 0000-0002-0183-6315

Funding

The work was funded by the Deutsche Forschungsgemeinschaft (grant NI 643/4-2).

DOI: 10.1021/acsomega.8b03415
ACS Omega 2019, 4, 5471−5478

Notes

The authors declare no competing financial interest.

■ ACKNOWLEDGMENTS

We thank Ulrich Baumann (University of Cologne) for access to protein crystallography infrastructure and the staff of the ESRF in Grenoble (France) and of the EMBL outstation in Hamburg (Germany) for assistance with diffraction data collection. Research team EA 4446 is grateful to Aude Rollet and Thi Huong Nguyen for technical assistance (chemical part).

■ ABBREVIATIONS

CK2, casein kinase 2; CK2α, catalytic subunit of protein kinase CK2; CK2α', paralogous isoform of CK2α; CK2β, regulatory subunit of protein kinase CK2; PDB, protein databank

■ REFERENCES

(1) Manning, G.; Whyte, D. B.; Martinez, R.; Hunter, T.; Sudarsanam, S. The protein kinase complement of the human genome. *Science* **2002**, *298*, 1912−1934.

(2) Lou, D. Y.; Dominguez, I.; Toselli, P.; Landesman-Bollag, E.; O'Brien, C.; Seldin, D. C. The alpha catalytic subunit of protein kinase CK2 is required for mouse embryonic development. *Mol. Cell. Biol.* **2008**, *28*, 131−139.

(3) Xu, X.; Toselli, P. A.; Russell, L. D.; Seldin, D. C. Globozoospermia in mice lacking the casein kinase II alpha' catalytic subunit. *Nat. Genet.* **1999**, *23*, 118−121.

(4) Niefind, K.; Guerra, B.; Ermakowa, I.; Issinger, O.-G. Crystal structure of human protein kinase CK2: insights into basic properties of the CK2 holoenzyme. *EMBO J* **2001**, *20*, 5320−5331.

(5) Guerra, B.; Issinger, O. G. Protein kinase CK2 in human diseases. *Curr. Med. Chem.* **2008**, *15*, 1870−1886.

(6) Cozza, G.; Pinna, L. A.; Moro, S. Protein kinase CK2 inhibitors: a patent review. *Expert Opin. Ther. Pat.* **2012**, *22*, 1081−1097.

(7) Hashimoto, A.; Gao, C.; Mastio, J.; Kossenkov, A.; Abrams, S. I.; Purandare, A. V.; Desilva, H.; Wee, S.; Hunt, J.; Jure-Kunkel, M.; Gabrilovich, D. I. Inhibition of casein kinase 2 disrupts differentiation of myeloid cells in cancer and enhances the efficacy of immunotherapy in mice. *Cancer Res.* **2018**, *78*, 5644−5655.

(8) Dowling, J. E.; Alimzhanov, M.; Bao, L.; Chuaqui, C.; Denz, C. R.; Jenkins, E.; Larsen, N. A.; Lyne, P. D.; Pontz, T.; Ye, Q.; Holdgate, G. A.; Snow, L.; O'Connell, N.; Ferguson, A. D. Potent and Selective CK2 Kinase Inhibitors with Effects on Wnt Pathway Signaling in Vivo. *ACS Med. Chem. Lett.* **2016**, *7*, 300−305.

(9) Siddiqui-Jain, A.; Drygin, D.; Streiner, N.; Chua, P.; Pierre, F.; O'Brien, S. E.; Bliesath, J.; Omori, M.; Huser, N.; Ho, C.; Proffitt, C.; Schwaebe, M. K.; Ryckman, D. M.; Rice, W. G.; Anderes, K. CX-4945, an orally bioavailable selective inhibitor of protein kinase CK2, inhibits prosurvival and angiogenic signaling and exhibits antitumor efficacy. *Cancer Res.* **2010**, *70*, 10288−10298.

(10) Bollacke, A.; Nienberg, C.; Le Borgne, M.; Jose, J. Toward selective CK2alpha and CK2alpha' inhibitors: Development of a novel whole-cell kinase assay by Autodisplay of catalytic CK2alpha'. *J. Pharm. Biomed. Anal.* **2016**, *121*, 253−260.

(11) Janeczko, M.; Orzeszko, A.; Kazimierczuk, Z.; Szyszka, R.; Baier, A. CK2α and CK2α' subunits differ in their sensitivity to 4,5,6,7-tetrabromo- and 4,5,6,7-tetraiodo-1H-benzimidazole derivatives. *Eur. J. Med. Chem.* **2012**, *47*, 345−350.

(12) Baier, A.; Nazaruk, J.; Galicka, A.; Szyszka, R. Inhibitory influence of natural flavonoids on human protein kinase CK2 isoforms: effect of the regulatory subunit. *Mol. Cell. Biochem.* **2018**, *444*, 35−42.

(13) Hochscherf, J.; Lindenblatt, D.; Witulski, B.; Birus, R.; Aichele, D.; Marminon, C.; Bouaziz, Z.; Le Borgne, M.; Jose, J.; Niefind, K. Unexpected Binding Mode of a Potent Indeno[1,2-b]indole-Type Inhibitor of Protein Kinase CK2 Revealed by Complex Structures with the Catalytic Subunit CK2α and Its Paralog CK2α'. *Pharmaceuticals* **2017**, *10*, 98.

(14) Alchab, F.; Ettouati, L.; Bouaziz, Z.; Bollacke, A.; Delcros, J.-G.; Gertzen, C. G. W.; Gohlke, H.; Pinaud, N.; Marchivie, M.; Guillon, J.; Fenet, B.; Jose, J.; Le Borgne, M. Synthesis, Biological Evaluation and Molecular Modeling of Substituted Indeno[1,2-b]indoles as Inhibitors of Human Protein Kinase CK2. *Pharmaceuticals* **2015**, *8*, 279−302.

(15) Hundsdörfer, C.; Hemmerling, H. J.; Götz, C.; Totzke, F.; Bednarski, P.; Le Borgne, M.; Jose, J. Indeno[1,2-b]indole derivatives as a novel class of potent human protein kinase CK2 inhibitors. *Bioorg. Med. Chem.* **2012**, *20*, 2282−2289.

(16) Bischoff, N.; Olsen, B.; Raaf, J.; Bretner, M.; Issinger, O. G.; Niefind, K. Structure of the human protein kinase CK2 catalytic subunit CK2α' and interaction thermodynamics with the regulatory subunit CK2β. *J. Mol. Biol.* **2011**, *407*, 1−12.

(17) Battistutta, R.; De Moliner, E.; Sarno, S.; Zanotti, G.; Pinna, L. A. Structural features underlying selective inhibition of protein kinase CK2 by ATP site-directed tetrabromo-2-benzotriazole. *Protein Sci.* **2001**, *10*, 2200−2206.

(18) Niefind, K.; Pütter, M.; Guerra, B.; Issinger, O. G.; Schomburg, D. GTP plus water mimic ATP in the active site of protein kinase CK2. *Nat. Struct. Biol.* **1999**, *6*, 1100−1103.

(19) Niefind, K.; Bischoff, N.; Golub, A. G.; Bdzhola, V. G.; Balanda, A. O.; Prykhod'ko, A. O.; Yarmoluk, S. M. Structural Hypervariability of the Two Human Protein Kinase CK2 Catalytic Subunit Paralogs Revealed by Complex Structures with a Flavonol- and a Thieno[2,3-d]pyrimidine-Based Inhibitor. *Pharmaceuticals* **2017**, *10*, 9.

(20) Ermakova, I.; Boldyreff, B.; Issinger, O.-G.; Niefind, K. Crystal structure of a C-terminal deletion mutant of human protein kinase CK2 catalytic subunit. *J. Mol. Biol.* **2003**, *330*, 925−934.

(21) Klopffleisch, K.; Issinger, O.-G.; Niefind, K. Low-density crystal packing of human protein kinase CK2 catalytic subunit in complex with resorufin or other ligands: a tool to study the unique hinge-region plasticity of the enzyme without packing bias. *Acta Crystallogr., Sect. D: Biol Crystallogr.* **2012**, *68*, 883−892.

(22) Ferguson, A. D.; Sheth, P. R.; Basso, A. D.; Paliwal, S.; Gray, K.; Fischmann, T. O.; Le, H. V. Structural basis of CX-4945 binding to human protein kinase CK2. *FEBS Lett.* **2011**, *585*, 104−110.

(23) Nakaniwa, T.; Kinoshita, T.; Sekiguchi, Y.; Tada, T.; Nakanishi, I.; Kitaura, K.; Suzuki, Y.; Ohno, H.; Hirasawa, A.; Tsujimoto, G. Structure of human protein kinase CK2 alpha 2 with a potent indazole-derivative inhibitor. *Acta Crystallogr., Sect. F: Struct. Biol. Cryst. Commun.* **2009**, *65*, 75−79.

(24) Tsuyuguchi, M.; Nakaniwa, T.; Kinoshita, T. Crystal structures of human CK2α2 in new crystal forms arising from a subtle difference in salt concentration. *Acta Crystallogr., Sect. F: Struct. Biol. Commun.* **2018**, *74*, 288−293.

(25) Brear, P.; De Fusco, C.; Georgiou, K. H.; Francis-Newton, N. J.; Stubbs, C. J.; Sore, H. F.; Venkitaraman, A. R.; Abell, C.; Spring, D. R.; Hyvönen, M. Specific inhibition of CK2α from an anchor outside the active site. *Chem. Sci.* **2016**, *7*, 6839−6845.

(26) Battistutta, R.; Mazzorana, M.; Cendron, L.; Bortolato, A.; Sarno, S.; Kazimierczuk, Z.; Zanotti, G.; Moro, S.; Pinna, L. A. The ATP-binding site of protein kinase CK2 holds a positive electrostatic area and conserved water molecules. *Chembiochem* **2007**, *8*, 1804−1809.

(27) Laskowski, R. A.; Swindells, M. B. LigPlot+: multiple ligand-protein interaction diagrams for drug discovery. *J. Chem. Inf. Model.* **2011**, *51*, 2778−2786.

(28) Gozzi, G. J.; Bouaziz, Z.; Winter, E.; Daflon-Yunes, N.; Aichele, D.; Nacereddine, A.; Marminon, C.; Valdameri, G.; Zeinyeh, W.; Bollacke, A.; Guillon, J.; Lacoudre, A.; Pinaud, N.; Cadena, S. M.; Jose, J.; Le Borgne, M.; Di Pietro, A. Converting potent indeno[1,2-b]indole inhibitors of protein kinase CK2 into selective inhibitors of the breast cancer resistance protein ABCG2. *J. Med. Chem.* **2015**, *58*, 265−277.

(29) Iegre, J.; Brear, P.; De Fusco, C.; Yoshida, M.; Mitchell, S. L.; Rossmann, M.; Carro, L.; Sore, H. F.; Hyvönen, M.; Spring, D. R.

DOI: 10.1021/acsomega.8b03415
ACS Omega 2019, 4, 5471−5478

Second-generation CK2α inhibitors targeting the αD pocket. *Chem. Sci.* **2018**, *9*, 3041−3049.
(30) Raaf, J.; Klopffleisch, K.; Issinger, O.-G.; Niefind, K. The catalytic subunit of human protein kinase CK2 structurally deviates from its maize homologue in complex with the nucleotide competitive inhibitor emodin. *J. Mol. Biol.* **2008**, *377*, 1−8.
(31) Niefind, K.; Issinger, O.-G. Conformational plasticity of the catalytic subunit of protein kinase CK2 and its consequences for regulation and drug design. *Biochim. Biophys. Acta* **2010**, *1804*, 484−492.
(32) Gouron, A.; Milet, A.; Jamet, H. Conformational flexibility of human casein kinase catalytic subunit explored by metadynamics. *Biophys. J.* **2014**, *106*, 1134−1141.
(33) Srivastava, A.; Hirota, T.; Irle, S.; Tama, F. Conformational dynamics of human protein kinase CK2α and its effect on function and inhibition. *Proteins* **2018**, *86*, 344−353.
(34) Salvi, M.; Sarno, S.; Marin, O.; Meggio, F.; Itarte, E.; Pinna, L. A. Discrimination between the activity of protein kinase CK2 holoenzyme and its catalytic subunits. *FEBS Lett.* **2006**, *580*, 3948−3952.

DOI: 10.1021/acsomega.8b03415
ACS Omega 2019, 4, 5471−5478